J Mater Sci (2011) 46:6794–6800
DOI 10.1007/s10853-011-5638-x

Purification of hot-pressed ZrCO into ZrC by a laser treatment

F. Goutier · N. Glandut · P. Lefort

Received: 3 April 2011 / Accepted: 16 May 2011 / Published online: 4 June 2011

Abstract Pellets of zirconium oxycarbide $ZrC_{0.82}O_{0.14}$, obtained by hot pressing of zirconia and zirconium carbide, were irradiated by an ytterbium-doped fibre laser in argon atmosphere (incident power density = 24.7 kW cm^{-2}, beam diameter 0.7 mm). The surface of the samples, heated at 3300 °C and more, i.e. near the melting, released its oxygen, leading to the carbide $ZrC_{0.75}$ despite the presence of traces of oxygen in the cell of treatment (P_{O_2} estimated around 1 Pa). A mechanism is proposed for explaining this result, based on the thermodynamical stability of the carbide, higher at these temperature and oxygen pressure than the oxide. Oxygen of the oxycarbide evolved in the form of the gaseous species ZrO, while the grains of the oxycarbide, converted into the carbide, grew from 2 to 20 μm. Similarly, the traces of dioxygen present inside the treatment cell react with the carbide, giving ZrO (gas), and do not form any oxidised solid phase. This opens interesting future prospects in the field of the production of oxygen-free zirconium carbide powders.

Introduction

It has been shown recently that a simple laser treatment of porous carbide ZrC disks led to the rapid melting of the surface, giving a complete densification of this material up to ca. 50 μm deep. The authors indicated that the melting was not accompanied by any oxidation, even if the protective surrounding gas (argon) contained small quantities of oxygen [1]. This result was somewhat surprising since zirconium carbide is well known for being very reactive with oxygen from relatively low temperatures [2, 3]. A thermodynamic explanation was given, on the basis of the volatility diagram of ZrC, showing that, at its melting point (experimentally estimated at 3420 °C [4] and thermodynamically at 3532 °C [5]) and for oxygen partial pressures lower than 10 Pa, ZrC (liquid) is in equilibrium with ZrO (gas). This means that, even if traces of oxygen were present, in the surrounding atmosphere, during the melting of the samples, its reaction produces the gaseous oxide ZrO, and hence, this element does not enter the liquid. The cooling being very rapid, no oxidation occurred, and the solidification of the liquid ZrC provided fully dense and very pure zirconium carbide, at the surface of the pellets. The possibility of obtaining ZrC by a laser process, in spite of relatively high dioxygen partial pressure was confirmed very recently by the reaction of a carbon film on the surface of ZrO_2 under nitrogen (P_{N_2} = 600 kPa) [6].

Considering these results, instead of using the laser treatment for densifying the surface of ZrC, it appeared theoretically possible to purify oxygen-containing ZrC under laser, since ZrC (without oxygen) is the stable phase at temperatures about 3400 °C, provided that the oxygen pressure remains low (< around 10 Pa).

Consequently, the aim of this work was to verify experimentally this assumption on the basis of a study using the zirconium oxycarbide as starting material [7], in order to attempt removing the oxygen off the oxycarbide.

Experimental

Powders

Zirconium oxycarbide was prepared through the solid–solid reaction between the carbide ZrC and the dioxide ZrO_2.

F. Goutier · N. Glandut · P. Lefort (✉)
SPCTS, CNRS UMR 6638, Centre Européen de la Céramique, 12 rue Atlantis, 87068 Limoges, France
e-mail: pierre.lefort@unilim.fr

The zirconium carbide powder used was provided by CERAC (Milwaukee, WI, USA, 99.5% pure, 325 mesh) and the zirconium dioxide by Alfa Aesar GmbH & Co (Karlsruhe, Germany) (99+% (metals basis excluding Hf, 325 mesh, monoclinic), with hafnium dioxide as main impurity (2%)). The mixtures were made in Ligroin by using ultrasonic pulses with 10 mol% ZrO_2 (11.7 wt%) and 90 mol% ZrC (88.3 wt%). Figure 1 provides X-ray diffraction (XRD) patterns of both the starting powders, which corresponded to the JCPDS files no. 35-0784 for ZrC and 37-1484 for ZrO_2. On the basis of these patterns, the lattice parameter of the carbide was 0.4699 ± 0.0001 nm, which indicated that its composition could be $ZrC_{0.94}$ [8], as far as it was reputed to be oxygen-free, the effect of this element being a decrease of the lattice parameter [9, 10].

Samples characterisation

Solid phases were analysed by XRD using an X-ray Brüker D5000 diffractometer ($\lambda_{Cu} = 0.15406$ nm). The scanned angles (in 2θ scale) ranged between 25° and 120° with a step of 0.01° and a 0.3 s exposure time. The X-ray patterns were indexed by using the DIFFRAC+ software (Socabim) containing JCPDS files database. Surface samples were observed by Scanning Electron Microscopy (SEM Philips XL30) equipped with EDS facilities (EDAX®).

Hot pressing

The mixtures ZrC/ZrO_2 were introduced into a graphite die (diameter of 15 mm) coated with a thin layer of boron nitride to avoid any carbon diffusion. They were hot-pressed for 210 min under 40 MPa at 1815 °C in an argon flow. The pellets obtained are shown in the SEM micrograph of Fig. 2, for a fractured sample. Their density, determined by pycnometry (Accupyc II 1340, Micromeritics Inc), was 6.59 ± 0.01 g cm^{-3}.

Their XRD patterns, given in Fig. 1, identified the only f.c.c. phase ZrC, with peaks shifted towards the high angles, as seen in the inserts of Fig. 1 for the peaks (111) and (511), that is characteristic of the oxycarbide lattice, where oxygen partially replaced carbon (zirconium dioxide was not longer detected). The calculated lattice parameter was 0.4682 ± 0.0001 nm, corresponding to that of the oxycarbide $ZrC_{0.82}O_{0.14}$ [8–10]. On this basis, the calculated density was of 6.69 g cm^{-3}; compared to the experimental value (6.59 g cm^{-3}), it meant that the hot-pressed samples were nearly fully dense (relative density of 98.5%).

Laser process

The laser used was an ytterbium laser (IPG, Oxford, MA, USA; model LCF 100) with the following characteristics: continuous wave, TEM_{00}, wavelength of 1072 ± 10 nm. The maximum output power was 100 W, with a beam

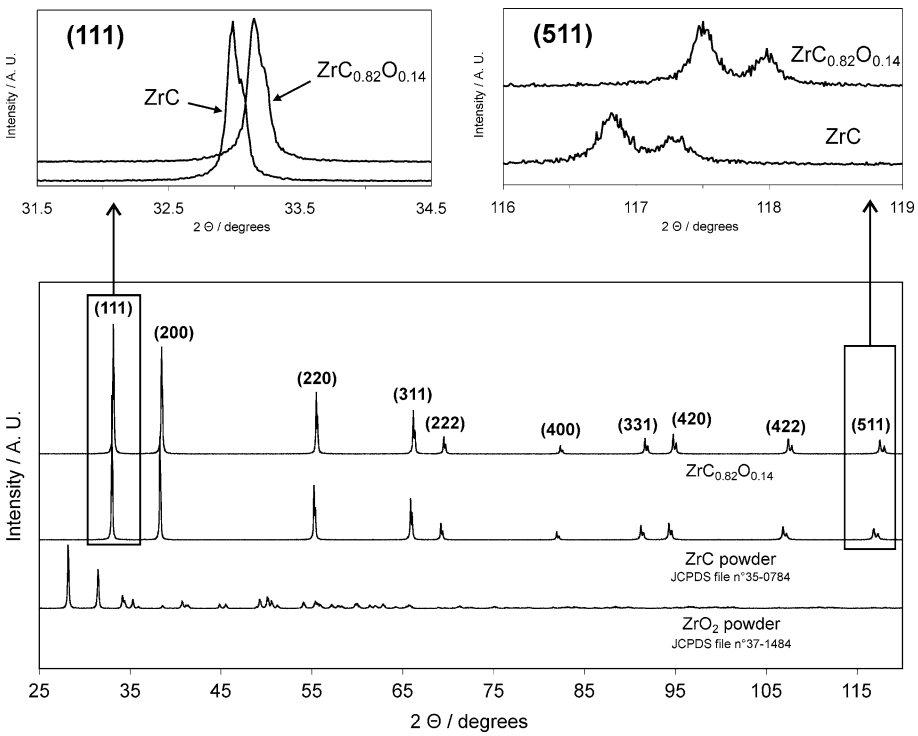

Fig. 1 XRD patterns of the starting powders and of the sintered zirconium oxycarbide

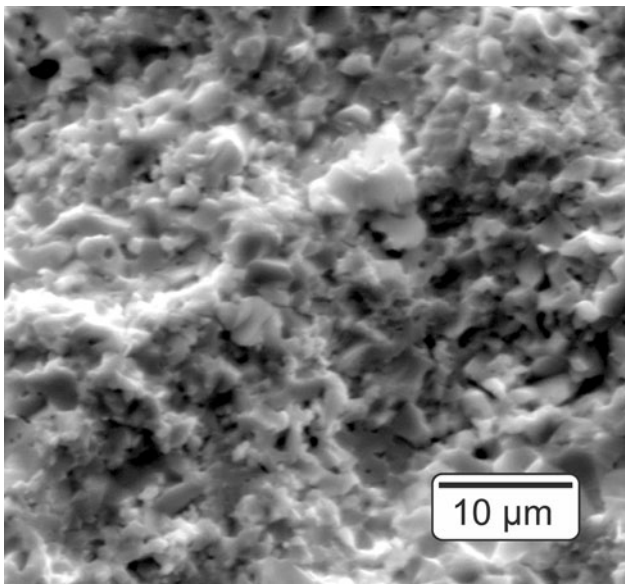

Fig. 2 SEM micrograph of the sintered zirconium oxycarbide (fracture)

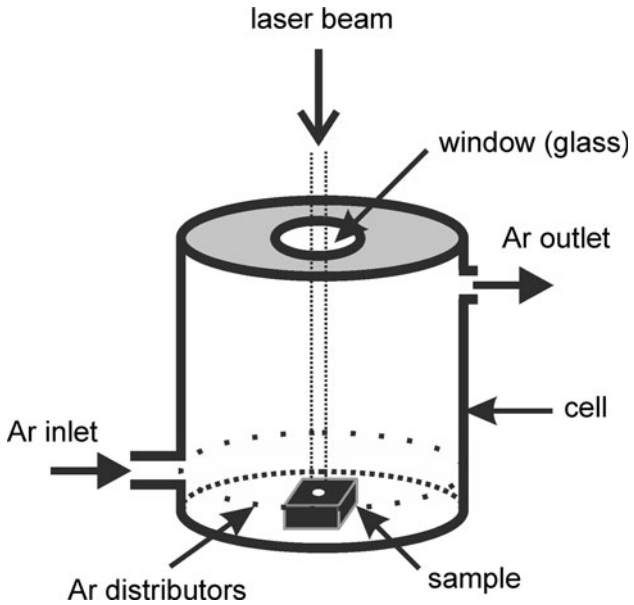

Fig. 3 Scheme of the cell used for the laser treatment

diameter of 5 mm (maximum power density of 509 W cm^{-2}). A beam reducer (Rodenstock, Germany) allowed reducing the beam diameter from 5 to 0.7 mm, without focusing. For the laser treatments, the samples were put in a cell filled with argon (flow rate around 2.8×10^{-4} m^3 s^{-1}), which isolated the sample from the ambient air during the laser process. The cell is schematically represented in Fig. 3.

The argon used ($[H_2O] < 3$ ppm; $[O_2] < 2$ ppm) was provided by Air Liquide, France (grade Alphagaz 1).

Results

In order to identify clearly the laser effect, a simple impact was realised on sintered samples, using a laser beam diameter of 0.7 mm. This method allows the SEM observation of the whole impact and the analysis by EDS of the treated zone simultaneously with the non-affected surface of the oxycarbide. Figure 4 presents the SEM observation and the EDS results obtained on a sample treated using the highest power density allowed by the process (beam diameter of 0.7 mm, with a power density of 24.7 kW cm^{-2}), for 90 s corresponding to an energy density of 2.2 MJ cm^{-2}. The choice of this high power was imposed, because the lower values modified only slightly the surface of the samples. This was probably due to the thermal diffusivity of the oxycarbide, supposed high, taking as a reference that of ZrC (45 W m^{-1} K^{-1} [11]), leading to a rapid dissipation of the heat at the periphery of the spot.

The impacted area appears dark and perfectly circular in Fig. 4a, with a diameter around 0.7 mm (740 µm between the two white dotted lines). All around the dark zone, a halo, clearer, is well visible, on a crown ca. 700 µm wide, and farther, the original oxycarbide is found.

The EDS profiles of the elements Zr, C and O (Fig. 4b), obtained along the bright transverse line of Fig. 4a show a relative increase of the Zr content inside and around the central zone, but mainly a deep depletion of oxygen (Fig. 4b) corresponding exactly to the dark area of Fig. 4a. At the opposite, a noticeable increase of this element is seen in the periphery of the dark zone, corresponding to the halo of Fig. 4a.

The estimated content of oxygen shows that this element has almost completely vanished in the dark zone that appears as composed only of zirconium and carbon: the mean atomic percentages of these elements (57.03% for Zr and 42.97% for C) give a composition $ZrC_{0.75}$ for the carbide. On the same basis, far from the spot, the mean atomic percentages provided by EDS (50.40% for Zr 7.97% for O and 41.63% for C) lead to an approximate composition of the oxycarbide $ZrC_{0.83}O_{0.16}$, close to that estimated by considering the lattice parameter. In the periphery of the dark zone, the mean atomic ratio O/Zr was 0.25, to be compared with the ratio O/Zr of 0.16 in the oxycarbide; here, the carbon content (36 at.%) was lower than in the rest of the sample, where it remained always quite constant, around 42 at.%.

The micrographs of Fig. 5 focus on the middle of the dark area, i.e. on the hottest zone of the sample. Figure 5a shows that the surface was crossed by several cracks and, in this zone, the scratches due to the rough polishing of the samples after the hot-pressing step, almost disappeared. Otherwise, the grains considerably grew, from an initial

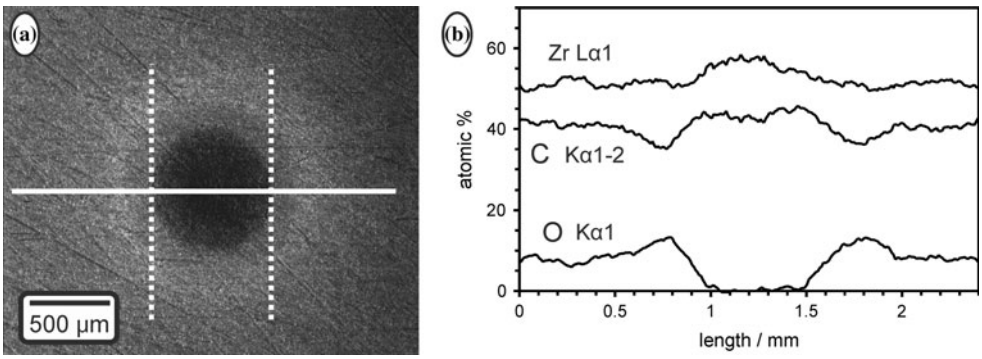

Fig. 4 Surface of a pellet of zirconium oxycarbide exposed during 90 s to a laser beam (**a**) (dark zone), and (**b**) EDS profiles along the bright line, for the elements Zr, C and O (Power = 24.7 kW cm^{-2}, beam diameter 0.7 mm)

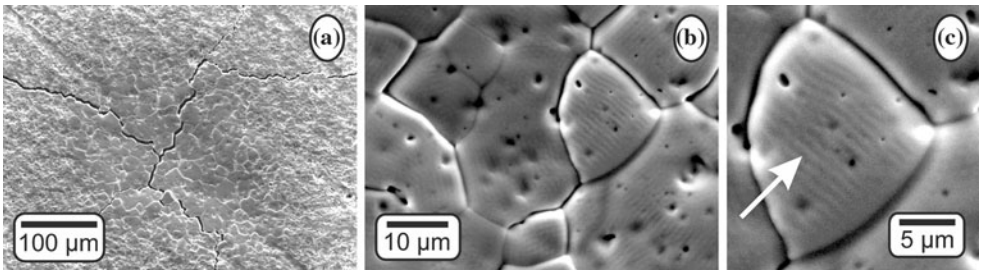

Fig. 5 Surface of a sample exposed 90 s under the laser beam (**a**) (power = 24.7 kW cm^{-2}, beam diameter 0.7 mm), with the detail of the surface of the grains (**b**) and a view of the ripples (**c**)

size of ca. 2 µm to more than 20 µm, with very well defined grain boundaries.

They were strewn by numerous pores, as it can be seen in Fig. 5b, corresponding to an open porosity that did not exist before the laser exposition. Lastly, a fine observation of the grains, such as in Fig. 5c revealed that their surface was not perfectly plane, but that it presented undulations parallel to one of the grain boundaries, the distance between two waves being always the same, close to 1.07 µm, that is the wavelength of the laser radiations.

Discussion

The whole results validate fully the hypothesis that was at the origin of the present work. Indeed, the oxycarbide heated at high temperature by a laser beam released its oxygen, so that the elements zirconium and carbon remained alone in the samples, so producing the carbide ZrC_{1-x}. Actually one may consider that this treatment purified the carbide, as far as oxygen could be considered as an impurity. It can be noticed that this result was obtained after very short treatment (90 s), and for depths superior to 1 µm, which correspond approximately to the thickness of the zone analysed by EDS. It would have been interesting knowing exactly the depth of the "purified" zone, but the treated samples were brittle and did not allow EDS analyses reliable for cross-sections. In the same way, the exact level of purification could not been determined precisely, insofar as quantifying the residual oxygen, if it exists, would have required a specific study. Nevertheless, the EDS results allow estimating its content, close to 1 at.%, or lower than this value, at the level of the surface.

There are two possible origins for the cracking observed. A first possibility is that it was due to the change of lattice parameter of the f.c.c. phase when oxygen evolved, which passed from 0.4682 nm (value determined for the oxycarbide) to 0.4701 nm (value estimated from [8] by considering the composition of the carbide $ZrC_{0.75}$ in the central zone). Nevertheless, this seems unlikely, because the consequence would have been an increase of the volume of the material located in the dark zone, and cracks would have appeared mainly at its periphery, not inside it, as seen in Fig. 5a where they share the grains along their boundaries. At the opposite, such a feature is characteristic of the crackles resulting from a thermal shock: indeed this zone cooled from temperatures higher than 3000 °C to around 500 °C in only a few seconds, when the laser irradiation stopped, the temperature of the rest of the surface remaining quite the same all along this time. Hence, the thermal origin of the cracking appeared by far the most likely.

About the temperature reached in the central part of the irradiated zone, it could not be measured, but it can be estimated by considering the facies of the surface grains. Contrary to what was described by Bacciochini et al. [1], no melting was observed (Figs. 4, 5), (if temperature had rose up to the melting, after cooling at room temperature,

the surface would have kept the aspect of a liquid congealed, seen the rapidity of cooling). Nevertheless, the grain growth, obtained in only 90 s, indicates a temperature near of 3420 °C (approximate ZrC_{1-x} melting point [4]). This is confirmed by the ripples structure seen in Fig. 5c: such a periodicity of the ripples, close to the wavelength of the laser beam, has already been described as characteristic of laser treatments of surfaces near the melting [12]. Consequently, the temperature reached by the surface of the dark area could be evaluated at least at 3300–3400 °C, but below 3420 °C. For temperatures like these, the atomic moves may also justify the fading observed of the polishing scratches.

Now, it is worth proposing a reaction mechanism for explaining the "purification" of the oxycarbide into the carbide. It is directly drawn from the previous work of Bacciochini et al. [1]. Let us consider, first, the system Zr/ZrO_2 from a thermodynamical point of view.

For this, the volatility diagram of this system is reported in Fig. 6. Details about building this kind of diagrams are given in literature [13–15]; Fig. 6 represents the stability domains of the different phases that could exist at 3327 °C (3600 K), on the basis of thermodynamical tables [5]. The condensed phases are thermodynamically stable inside the zones delimited by the solid lines, according to the partial pressure of oxygen P_{O_2}. For instance, for $P_{O_2} = 1$ Pa ($\log P_{O_2} = 0$), the condensed stable phase is ZrO_2 (liquid) alone, and it is in equilibrium with the gaseous phase ZrO with a rather high partial pressure ($P_{ZrO} = 10^{3.76}$ Pa = 5.75×10^3 Pa). It is worth noticing that, for the gaseous species, the boundaries delimit only predominance domains; it is the reason why the separations are drawn in dotted line (e.g. always for $P_{O_2} = 1$ Pa, the gaseous species that emerge from ZrO_2 (liquid) is $ZrO_{(g)}$ alone, but $ZrO_{(g)}$ partially converts into $Zr_{(g)}$ and $ZrO_{2(g)}$, in gaseous phase, even if the thermodynamical calculations indicate that $ZrO_{(g)}$ remains the predominant species).

The partial pressure of oxygen considered above (1 Pa) is realist experimentally, in the cell of treatment, since it is lower in the argon used (0.2 Pa), but taking into account a possible lack of gastightness of the cell. (Nevertheless, one may consider that, with an argon flow rather high, around 2.8×10^{-4} m^3 s^{-1}, seen the small size of the cell, which was in superpressure, the penetration of oxygen from the exterior was probably very limited.) However that may be, the temperature being supposed reaching about 3300 °C, and the partial pressure of oxygen being supposed as fixed around 0.2–1 Pa by the argon flow, seen the Fig. 6, if ZrO_2 was present on the sample:

(i) It was liquid and in equilibrium with $ZrO_{(g)}$, this being true in a large range of oxygen partial pressures ($3 \times 10^{-2} < P_{O_2} < 21$ Pa);
(ii) The partial pressure of $ZrO_{(g)}$ was rather high ($2.8 \times 10^4 < P_{ZrO} < 1.3 \times 10^3$ Pa, according to the partial pressures of oxygen above);
(iii) And the evaporation of ZrO_2 giving $ZrO_{(g)}$ was certainly intense, because of the high argon flow rate in the cell;

so that, if ZrO_2 existed, it vanished certainly very quickly.

About the carbide, the volatility diagram of Fig. 7, established on the basis of the same thermodynamical tables [5], shows that it is the solid phase stable at 3327 °C, provided that P_{O_2} is lower than 5 Pa that is true in the experimental conditions discussed above. Consequently, oxygen present in the cell may react with the carbide (always for a pressure of 1 Pa), giving $ZrO_{(g)}$ and $CO_{(g)}$ by:

$$ZrC\,(s) + O_2\,(g) = ZrO\,(g) + CO\,(g) \quad (1)$$

but not any oxidation inside the carbide (solid) was possible.

Now, at these temperature and oxygen pressure, the oxycarbide can be thermodynamically considered as the sum of Zr (liquid), ZrC (solid) and ZrO_2 (liquid) (Eq. 2):

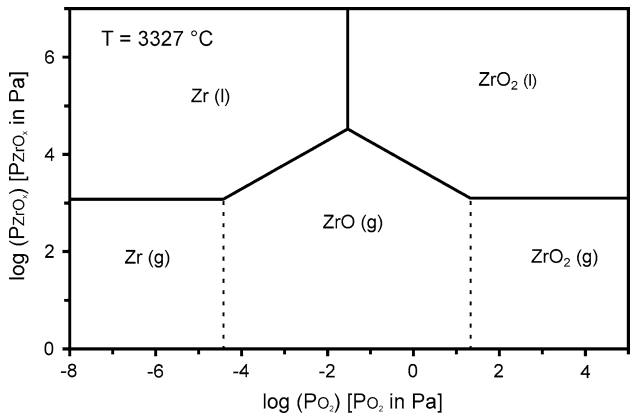

Fig. 6 Volatility diagram for the system Zr–O at 3327 °C (thermodynamical data from Ref. [5])

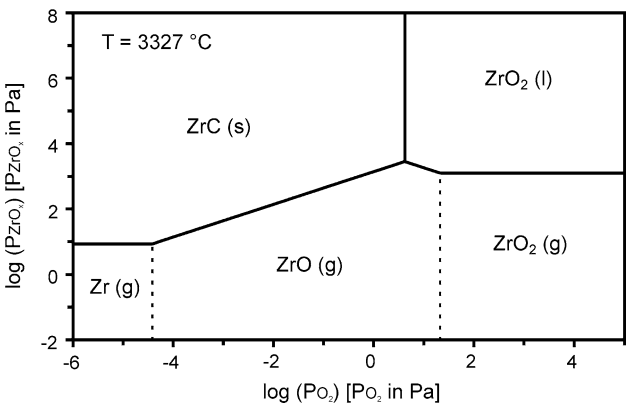

Fig. 7 Volatility diagram for the system Zr–O–C at 3327 °C (thermodynamical data from Ref. [5])

$$ZrC_{0.82}O_{0.14} = 0.11\,Zr + 0.82\,ZrC + 0.07\,ZrO_2 \quad (2)$$

So, globally and by referring to Figs. 6 and 7, the following reactions must occur, in ca. 1 Pa of oxygen around 3300 °C:

$$Zr\,(l) + \frac{1}{2}O_2\,(g) \rightarrow ZrO\,(g)\ (\text{out of equilibrium, hence likely very rapid}) \quad (3)$$

$$Zr\,(l) + \frac{1}{2}O_2\,(g) \rightarrow ZrO_2\,(l)\ (\text{out of equilibrium, hence likely very rapid}) \quad (4)$$

$$ZrO_2\,(l) \rightarrow ZrO\,(g) + \frac{1}{2}O_2\,(g) \quad (5)$$

and

$$ZrC\,(s) + O_2\,(g) = ZrO\,(g) + CO\,(g) \quad (1)$$

The effect of these reactions is the release of oxygen off the oxycarbide, and the formation of pure carbide ZrC, even despite the presence of traces of oxygen in the cell.

Such a mechanism is consistent with all the observed features, in particular:

(i) It justifies the release of oxygen off the oxycarbide;
(ii) It explains the presence of a halo rich in oxygen around the dark central zone: ZrO (gas) evolving during the treatment, arrives very hot on the much colder part around the zone irradiated by the laser beam. It must condense, forming ZrO_2 that is the only stable solid phase oxide in the system Zr–O. However, the value of the ratio O/Zr determined by EDS was not equal to 2 (as in ZrO_2) but to 0.25 only. Considering the depth of EDS analyses (ca. 1 μm) it means that the thickness of ZrO_2 must be very low in the halo, the analyses taking into account both the thin scale of ZrO_2 and the underlying oxycarbide $ZrC_{0.82}O_{0.14}$. This mechanism is described schematically in Fig. 8;
(iii) It is consistent with the appearance of porosity inside the grains of ZrC: ZrO (gas) must leave the almost fused carbide, and the porosity observed may perfectly be the ways for evolving this gas.

Conclusion

From a practical point of view, it appears possible, now, to purify zirconium carbide having relatively high contents of oxygen as main impurity, by an appropriate laser treatment (time exposure, controlled atmosphere). This could have applications, for instance such a treatment could accelerate the last stage of the carbothermal reduction of zirconia, which produces rapidly the oxycarbide $ZrC_{0.84}O_{0.06}$, first, and then, slowly, the carbide [15, 16].

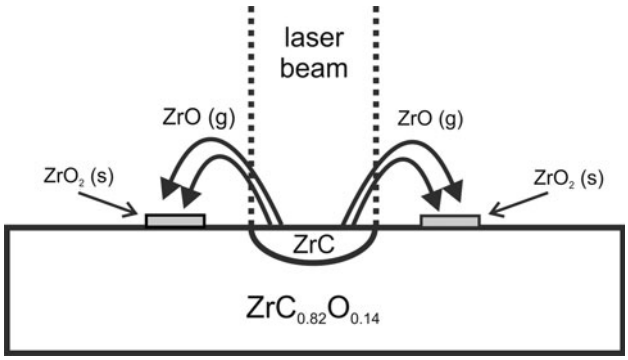

Fig. 8 Scheme of the volatilisation and condensation of ZrO

Nevertheless, this study has shown that this process is not really convenient for fully dense samples, because of the thermal shock associated to the very rapid heating and cooling of the surfaces, associated with the laser use. It creates cracks on the samples, often with disastrous consequences for the pieces. This process must probably be retained principally for the surface treatment of porous materials, less sensible to thermal shocks, or maybe for powders, especially for the elaboration of carbide ZrC with a high purity in view of its sintering [17–20].

Lastly, it is likely that other carbides or borides could be purified by this way, provided that they remain stable at very high temperatures.

References

1. Bacciochini A, Glandut N, Lefort P (2009) J Eur Ceram Soc 29:1507
2. Shimada S (2002) Solid State Ionics 149:319
3. Hou X-M, Chou K-C (2011) J Alloys Compd 509:2395
4. Guillermet AF (1995) J Alloys Compd 217:69
5. Chase MW Jr, Davies CA, Downey JR Jr, Frurip DJ, McDonald RA, Syverud AN (1986) JANAF thermochemical tables. American Ceramics Society, New York
6. Yilbas BS, Akhtar SS, Karatas C (2011) Appl Surf Sci. 257:6912. doi:10.1016/j.apsusc.2011.03.030
7. Min-Haga E, Scott WD (1988) J Mater Sci 23:2865. doi:10.1007/BF00547460
8. Storms EK (1967) Refractory materials: the refractory carbides, vol 2. Academic Press, New York
9. Ouensanga A, Dode M (1976) J Nucl Mater 59:49
10. Barnier P (1986) Frittage et caractérisation de céramiques dans le système zirconium-carbone-oxygène. Thesis, Ecole Nationale Supérieure des Mines, Saint Etienne, France
11. Storms EK, Wagner P (1973) High Temp Sci 5:454
12. Kolasinski KW (2007) Curr Opin Solid State Mater Sci 11:76
13. Heuer AH, Lou VLK (1990) J Am Ceram Soc 73:2785
14. Lefort P, Tetard D, Tristant P (1993) J Eur Ceram Soc 12:123

15. Maître A, Lefort P (1997) Solid State Ionics 104:109
16. Sacks MD, Wang C-A, Yang Z, Jain A (2004) J Mater Sci 39:6057. doi:10.1023/B:JMSC.0000041702.76858.a7
17. Alexandrescu R, Borsella E, Botti S, Cesile MC, Martelli S, Giorgi R, Turtù S, Zappa G (1997) J Mater Sci 32:5629. doi:10.1023/A:1018640911556
18. Zhao D, Hu H, Zhang C, Zhang Y, Wang J (2010) J Mater Sci 45:6401. doi:10.1007/s10853-010-4722-y
19. Zhao L, Jia D, Duan X, Yang Z, Zhou Y (2011) Int J Refract Metals Hard Mater 29:516
20. Wang X-G, Guo W-M, Kan Y-M, Zhang G-J, Wang P-L (2011) J Eur Ceram Soc 31:1103